Sediment fingerprinting as a tool for interpreting long-term river activity: The Voidomatis basin, Northwest Greece

Edited by
Ian D L Foster

Tracers in Geomorphology

WILEY

25 Sediment Fingerprinting as a Tool for Interpreting Long-term River Activity: The Voidomatis Basin, North-west Greece

R. H. B. HAMLIN,[1] J. C. WOODWARD,[1] S. BLACK[2] and M. G. MACKLIN[3]
[1]*School of Geography, University of Leeds, UK*
[2]*PRIS, University of Reading, UK*
[3]*Institute of Geography and Earth Sciences, University of Wales, Aberystwyth, UK*

INTRODUCTION

Information on sediment provenance is a fundamental requirement for many geological and geomorphological investigations. Provenance data have been used to calibrate models of tectonic uplift and displacement, to investigate the formation of sedimentary sequences and for large-scale palaeogeographic reconstructions (Haughton *et al.*, 1991). Within process geomorphology provenance information has proved to be of considerable value in elucidating catchment sediment dynamics, providing information on temporal and spatial variations in sediment sources (e.g. Yu and Oldfield, 1989; Walling and Woodward, 1995; Collins *et al.*, 1998). These studies have focused mainly on either tracing the source of contemporary suspended sediment (e.g. Walling *et al.*, 1979; Walling and Woodward, 1992, 1995) or on fine-grained sediments deposited in lake basins and estuaries (e.g. Yu and Oldfield, 1989, 1993; Dearing, 1992; Hutchinson, 1995). They have demonstrated that the source of sediment from catchment areas of contrasting land use and/or lithology can be established (e.g. Walling and Woodward, 1995).

Many provenance studies have employed qualitative or semi-quantitative methods to identify sediment source areas or types (e.g. Wood, 1978; Walling *et al.*, 1979; Oldfield *et al.*, 1985; Woodward *et al.*, 1992). More recently, however, techniques for obtaining more robust, quantitative constraints of fine sediment source have been developed. These 'quantitative fingerprinting' approaches (Peart and Walling, 1986) assume that the physical and chemical properties of the sediment of interest directly reflect the relative contributions from catchment source areas. Certain physical and chemical properties are first selected to differentiate the source area materials (soils, sediments, bedrock, etc.), and then a multivariate mixing model is used to determine the relative contribution of each individual source type (e.g. Walling *et al.*, 1993; Yu

Tracers in Geomorphology. Edited by Ian D. L. Foster.

and Oldfield, 1989). A wide variety of approaches have been employed to establish sediment provenance, including geochemistry (Passmore and Macklin, 1994; Collins *et al.*, 1997a,b, 1998), mineral magnetics (Walling *et al.*, 1979; Yu and Oldfield, 1989, 1993; Dearing, 1992; Hutchinson, 1995; Foster *et al.*, 1998), radionuclide concentrations (Walling and Woodward, 1992; Olley *et al.*, 1993; Hutchinson, 1995), SEM analysis (de Boer and Crosby, 1995), mineralogy (Wood, 1978; Woodward *et al.*, 1992), sediment colour (Grimshaw and Lewin, 1980) and particle-size distributions (Kurashige and Fusejima, 1997).

Whilst there has been some work on sourcing Holocene floodplain deposits (Woodward *et al.*, 1992; Passmore and Macklin, 1994; Collins *et al.*, 1997b; Schell *et al.*, see Chapter 26), the potential for *quantitative* provenancing in elucidating long-term changes (10^2–10^5 years) in fine sediment sources remains largely undocumented. Over these timescales, the flux and provenance of fine-grained fluvial sediment may be influenced by environmental controls such as climate variations, vegetation dynamics, land-use change or tectonic activity. Thus data on changes in Late Pleistocene and Holocene sediment provenance may provide valuable information on long-term river behaviour and catchment dynamics. This study applies a quantitative fingerprinting technique to Pleistocene and Holocene fluvial deposits in the Voidomatis basin, a steepland catchment in north-west Greece. Results are presented for both the chronology and provenance of the fine-grained matrix within coarse alluvial fills, and fine-grained palaeoflood slackwater deposits (SWDs). The chapter builds on previous work in the area (Woodward *et al.*, 1992) to explore the variation in sediment sources during and since the Late Pleistocene, and how this may be related to long-term environmental change.

STUDY AREA: PHYSICAL CHARACTERISTICS AND PREVIOUS RESEARCH

The Voidomatis River basin (384 km^2) drains the western side of the Pindus Mountains in Epirus, north-west Greece (Figure 25.1). The river is steep (average gradient 0.016), with elevations within the catchment ranging from over 2400 m along the watershed to *c.* 390 m on the Konitsa basin (Lewin *et al.*, 1991). River incision driven by long-term tectonic uplift has resulted in the development of deep bedrock gorges (Figures 25.1 and 25.2). The largest of these is the Upper Vikos Gorge which reaches depths of almost 1000 m (Bailey *et al.*, 1997). Immediately downstream the Voidomatis flows through the Lower Vikos Gorge and out into the Konitsa basin (Figure 25.1). In the Lower Vikos Gorge the Voidomatis is a 10–20 m wide, meandering gravel-bed river, with extensive bars and prominent riffles.

Rainfall is concentrated from October to May. Intense and prolonged storms are common, and daily rainfall totals of over 115 mm have been recorded. Mean annual precipitation ranges from 1079 mm over the Lower Vikos Gorge to 1702 mm in the particularly mountainous Tsepelovon area (Figure 25.1).

Alluvial fills in the lower part of the basin display two distinctive types of lithofacies. First, high units 8–15 m above the modern channel are quite frequently preserved, especially in wider gorge sections where there has been less reworking.

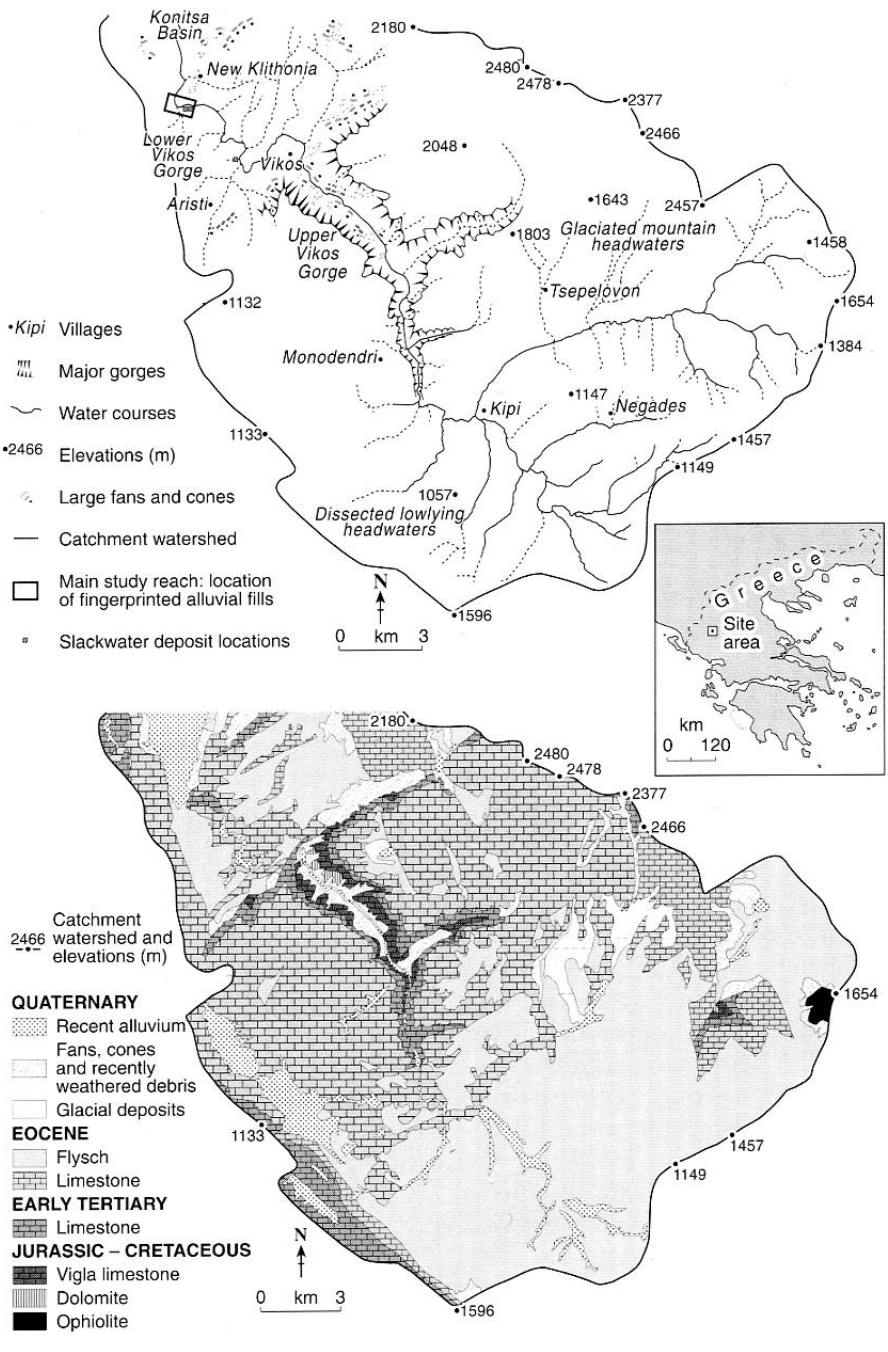

Figure 25.1 Maps of the Voidomatis catchment showing physical characteristics, study sites and geology (after IGME, 1968, 1970). (*Terra rossa* occurs as a thin soil on top of some of the exposed limestone areas. Dolomite-enriched flysch is present in the extreme east of the catchment)

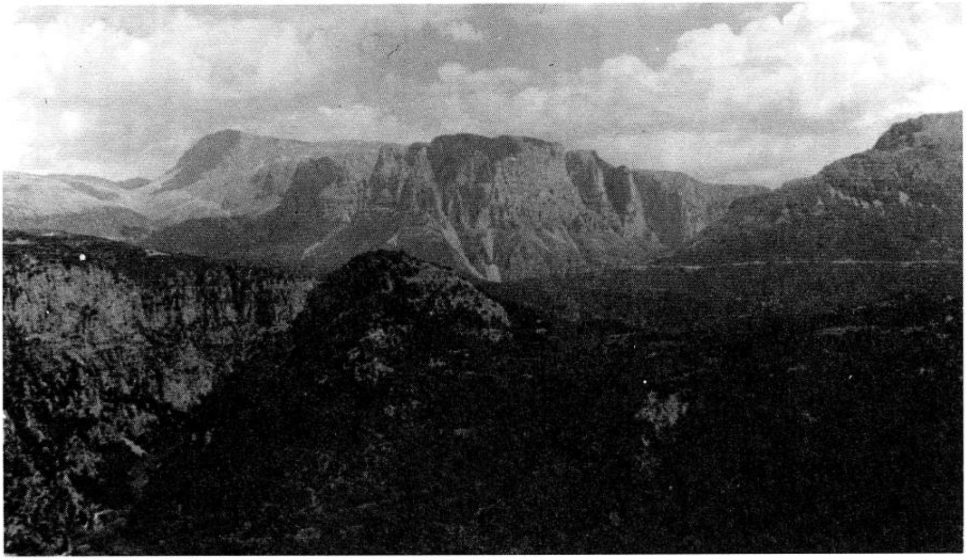

Figure 25.2 The Voidomatis catchment with the Lower Vikos Gorge evident in the foreground and the Upper Vikos Gorge in the background

These alluvial units are composed of well-rounded coarse gravels and small boulders in a fine-grained sandy matrix. Secondly, in near-channel areas lower units exist approximately 2–4 m above the modern channel, composed of coarse sandy gravel overlain by thick deposits of bedded sands and silts. Previous work in the area (Lewin *et al*., 1991) has subdivided the chronology of the older, coarse-grained sediments into the Late Pleistocene Aristi (*c*. 28 200 (±7000) to 24 300 (±2600) years BP) and Vikos (*c*. 24 300 (±2600) to 19 600 (±3000) years BP) units (Woodward *et al*., 1992). In addition, a very old (>150 000 years BP) Kipi unit was also identified in the upper part of the catchment (Lewin *et al*., 1991), but this is not discussed here. The younger, predominantly fine-grained sediments were termed the Klithi unit, and whilst this unit was shown to be composite in nature, its deposition was dated to the last 1000 years (Lewin *et al*., 1991). Dating was achieved by means of ESR, TL and ^{14}C (Lewin *et al*., 1991), whilst clast lithological analysis and semi-quantitative sourcing of the fine (<63 μm) fraction confirmed the differences between these alluvial units (Woodward *et al*., 1992). Investigation of soil development on these units identified that there were at least two different phases of Late Pleistocene Aristi-type sedimentation, the more recent at *c*. 28 200 (±7000) to 24 300 (±2600) years BP, and an earlier phase of sedimentation with a minimum age of *c*. 85 000 years, estimated by means of a soil weathering index (Woodward *et al*., 1994). The palaeoenvironmental implications of these results have been discussed in detail by Macklin *et al*. (1997). We have now extended that work by mapping and surveying parts of the valley floor in detail, and by applying recent developments in radiometric dating and fine sediment fingerprinting to the alluvial deposits of the Voidomatis basin.

In addition to the major valley-floor alluvial units, fine-grained palaeoflood slackwater deposits (SWDs) have been identified at three locations in the catchment

(Figure 25.1) (Lewin *et al.*, 1991). These sequences present an opportunity to investigate the occurrence and significance of high-magnitude floods over the Late Pleistocene, which has rarely been explored in the Mediterranean region. It is well known that extreme flood events can play an important role in valley-floor development (e.g. Baker, 1977; Gupta, 1983; Coxon *et al.*, 1996), especially in high threshold environments. SWDs are typically fine-grained sediment sequences ($D_{50} < 2$ mm), resulting from the rapid deposition of suspended sediment during large floods in sheltered areas, where flow velocities suddenly decrease and reverse eddying predominates (Baker *et al.*, 1983). Much of the previous work on such sedimentary features has been in the USA (Kochel and Baker, 1982, 1988; Ely and Baker, 1985; O'Connor *et al.*, 1994; Ely, 1997) and Australia (Baker and Pickup, 1987; Gillieson *et al.*, 1991; Wohl, 1992; Saynor and Erskine, 1993), with only very recent work providing detailed analysis of SWDs in the Mediterranean region (cf. Benito *et al.*, 1998; Greenbaum *et al.*, 1998). The stable channel cross-sections and large river stage increases during floods in the gorges of the Voidomatis basin are conducive to the long-term preservation of these deposits. They have been identified in areas of ineffective flow during large floods, such as tributary mouths, areas of channel expansion and in the floor of rockshelters and caves, preserved at 9–11 m above the channel bed.

FIELD AND LABORATORY METHODS

Study Sites and Dating Techniques

Geomorphological mapping and surveying techniques were employed to identify the number, extent and height of river terraces. A reach encompassing the southern corner of the Konitsa basin and the mouth of the Lower Vikos Gorge was selected for detailed study (Figure 25.1) as it contained extensive, well-preserved terrace surfaces with good exposures in river cut sections. It was common to find the coarse-grained Late Pleistocene alluvial fills cemented by calcite as a result of the carbonate-rich character of the surrounding bedrock. This accumulation of secondary calcite has firmly cemented clasts of all sizes, normally within the upper 1–1.5 m of the sediments. The calcite formation was dated by means of uranium-series disequilibria ($^{230}Th/^{234}U$ method) and provides a minimum age for the alluvial deposits. Uranium-series radionuclides were measured by high-resolution alpha spectrometry and ICP-MS at Lancaster University. Uranium and thorium isotopes were separated on ion-exchange resins and electrodeposited onto stainless steel planchets (see Black *et al.*, 1997; Kuzucuoglu *et al.*, 1998). Corrections were made for decay of excess ^{234}U and detrital ^{230}Th, on the assumption that these were present at precipitation of the calcite deposits. A correction for the detrital component was made from isochron plots after successive total dissolutions were performed, following the methods of Bischoff and Fitzpatrick (1991). In all cases the slopes of the isochrons are best determined by a method of least-squares fitting which takes account of the errors in both variables (after York, 1969).

Three main sites with SWDs have so far been identified within the catchment. These are the Boila and Old Klithonia Bridge sites at the bottom of Lower Vikos Gorge, and the Tributary site which is located in a left bank tributary in the middle reaches of the Lower Vikos Gorge, just upstream of the Spiliotissa Monastery (Figure 25.1). Dating of the Boila sediments was achieved by AMS ^{14}C analysis of charcoal, whilst a vein of cemented sands in the Tributary site SWDs yielded a uranium-series age.

Field Sampling

For the fingerprinting procedure, 52 source samples were collected from all major geological formations within the catchment (Figure 25.1). Target samples were then collected from all the deposits of interest. Two samples of fine sediment were taken from each alluvial unit. Material was collected from different parts of naturally exposed sections in an attempt to account for any heterogeneity in sediment properties. In the case of the cemented alluvial units, care was taken to ensure that these were collected from the lower, unconsolidated parts of the sediments which were free from alteration by secondary calcite and pedogenic weathering (Woodward *et al.*, 1992, 1994). The SWDs were logged in detail, and samples were carefully collected from each sedimentary layer. Samples of contemporary fluvial fines were collected from channel margin locations at eight sites along the main channel.

Determination of Fine Sediment Properties

A combination of geochemical and magnetic analyses was chosen to quantify the differences between source materials, as they can provide reliable quantitative information for a number of independent parameters. The use of two contrasting types of sediment property, which reflect different environmental controls, is likely to yield more reliable fingerprinting results (Walling *et al.*, 1993).

For geochemical analyses, the < 2 mm fraction of the source materials and target sediments was used. The trace elements Ba, Cu, Cr, La, Nd, Ni, Pb, Rb, Sr, V, Y, Zn and Zr were determined by X-ray fluorescence (XRF) using a ARL 9400 spectrometer. Both low-frequency specific magnetic susceptibility (χ) and frequency-dependent magnetic susceptibility ($\chi_{FD}\%$) were determined for the <1 mm sample fraction using a standard Bartington MS2 magnetic susceptibility meter. Magnetic susceptibility is largely a function of the concentration of ferrimagnetic minerals, particularly magnetite (Fe_3O_4) (Thompson and Oldfield, 1986), although it is also sensitive to changes in magnetic grain size. Frequency-dependent magnetic susceptibility, however, is largely a function of the concentration of ultrafine ($<0.03\,\mu m$) superparamagnetic grains within the sample (Dearing, 1994).

ALLUVIAL STRATIGRAPHY AND CHRONOLOGY

Phases of Aggradation and Incision

Geomorphological mapping and survey work in the southern part of the Konitsa basin (main study reach, Figure 25.1) has identified a series of river terraces and palaeochannels. The broad valley floor at this point has facilitated good preservation of alluvial sediments. Five high (15.5–8.5 m) coarse-grained alluvial units, and three lower (4.5–2.0 m) predominantly fine-grained units were identified (Figure 25.3). The coarse-grained units are equivalent to the previously described Aristi-type sediments (Lewin *et al.*, 1991). All but one contained an exposed cemented upper layer from which samples were taken for uranium-series dating. These yielded Late Pleistocene ages for these sediments, culminating in a depositional phase that ended at *c.* 25 000±2000 years BP (Figure 25.3). These dates provide a minimum age for the deposits, with the calcite cement assumed to have formed soon after the depositional

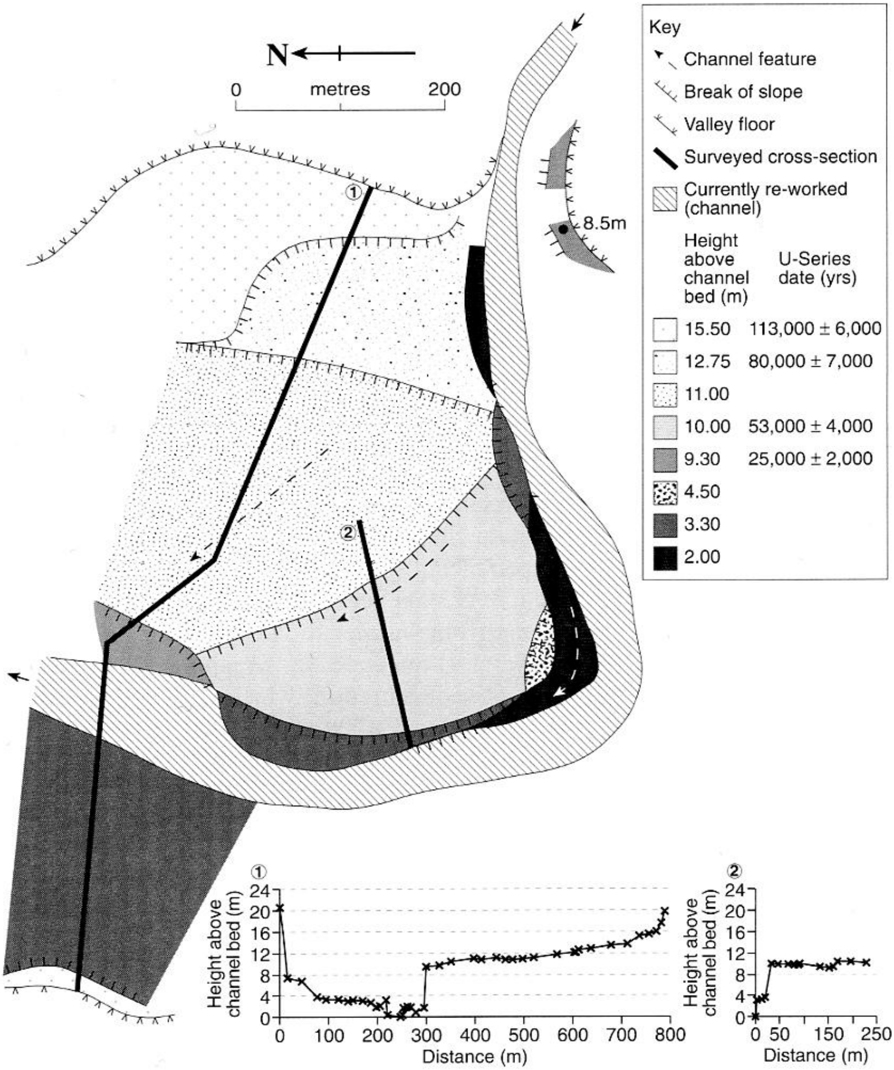

Figure 25.3 Geomorphological map of the Konitsa basin study reach (location shown on Figure 25.1)

phase of the detrital material. This is consistent with the observed U–Th isochrons which show very good correlations (r^2 >0.98) indicating that the cement probably formed during a short time period. These features therefore provide clear evidence for five phases of aggradation and incision over the Late Pleistocene, when the channel bed was between 8 and 15 m higher than at present. The lower units are Late Holocene alluvial fills, and represent the multi-phase Klithi unit sediments described by Lewin *et al.* (1991) and Woodward *et al.* (1994). Radiocarbon-dated charcoal from a preserved hearth buried within a unit of this type in the Lower Vikos Gorge yielded an age of AD 1420 to 1650 (Beta-109186). This hearth was overlain by >1.5 m of fine-grained overbank sediments.

These dates can be compared with climate proxy records. Three records have been selected for this study (see Figure 25.4): (i) the long pollen record from Lake Ioaninna (Tzedakis, 1994; Tzedakis *et al.*, 1997), only 30 km to the south of the Voidomatis basin; (ii) an oxygen isotope record from the central Mediterranean Sea (Paterne *et al.*, 1986); and (iii) the high-resolution GRIP oxygen isotope record (GRIP Members, 1993; Thouveny *et al.*, 1994). The dating results from the Konitsa basin reach are plotted with 2 sigma uncertainties and are shown with dates from alluvial units elsewhere in the Lower Vikos Gorge which exhibit notable similarities (Figure 25.4). These results demonstrate the following:

(1) A major phase of Late Pleistocene aggradation occurred at approximately 25 000 years BP, which on all palaeoclimate records is associated with the pronounced cold period of the Last Glacial Maximum (LGM) (Figure 25.4).
(2) The earlier phases of aggradation took place around 55 000, 78 000 and 113 000 years BP. Greater uncertainty with older dates can make correlation to environmental phases less precise, especially in view of the fluctuating and complex nature of Late Pleistocene climate change. However, it is likely that at 55 000 years BP the area was also experiencing cold conditions (early Oxygen Isotope Stage (OIS) 3), whilst 78 000 and 113 000 years BP seem to have been periods of transitional climate, changing from warmer to cooler periods (OIS 5a to 4 and OIS 5e to 5d, respectively) (Figure 25.4). Mapping in the Konitsa basin identified another phase of sedimentation, which although not directly dated, can be bracketed to between *c.* 80 000 and 53 000 years BP (Figure 25.3). All of these dated units represent major periods of Aristi-type aggradation.

Periods of High-Magnitude Flooding

The SWDs are laminations of sand and silt (e.g. Figures 25.5 and 25.6), typical of flood deposition in high-level slackwater zones. At the Boila rockshelter (Kotjaboupoulou *et al.*, 1997), a series of flood events occurred between 13 960 ± 260 (Beta-109162) and 14 310 ± 200 (Beta-109187) years BP (2 sigma uncertainties), overtopping the lip of the cave and depositing the flood sediments (Figures 25.5 and 25.6). This was an unstable period of climatic change encompassing warming after the LGM (Figure 25.4). A uranium-series date on the Tributary site SWDs of 21 250 ± 2500 years BP indicates the occurrence of large floods during the cold conditions of

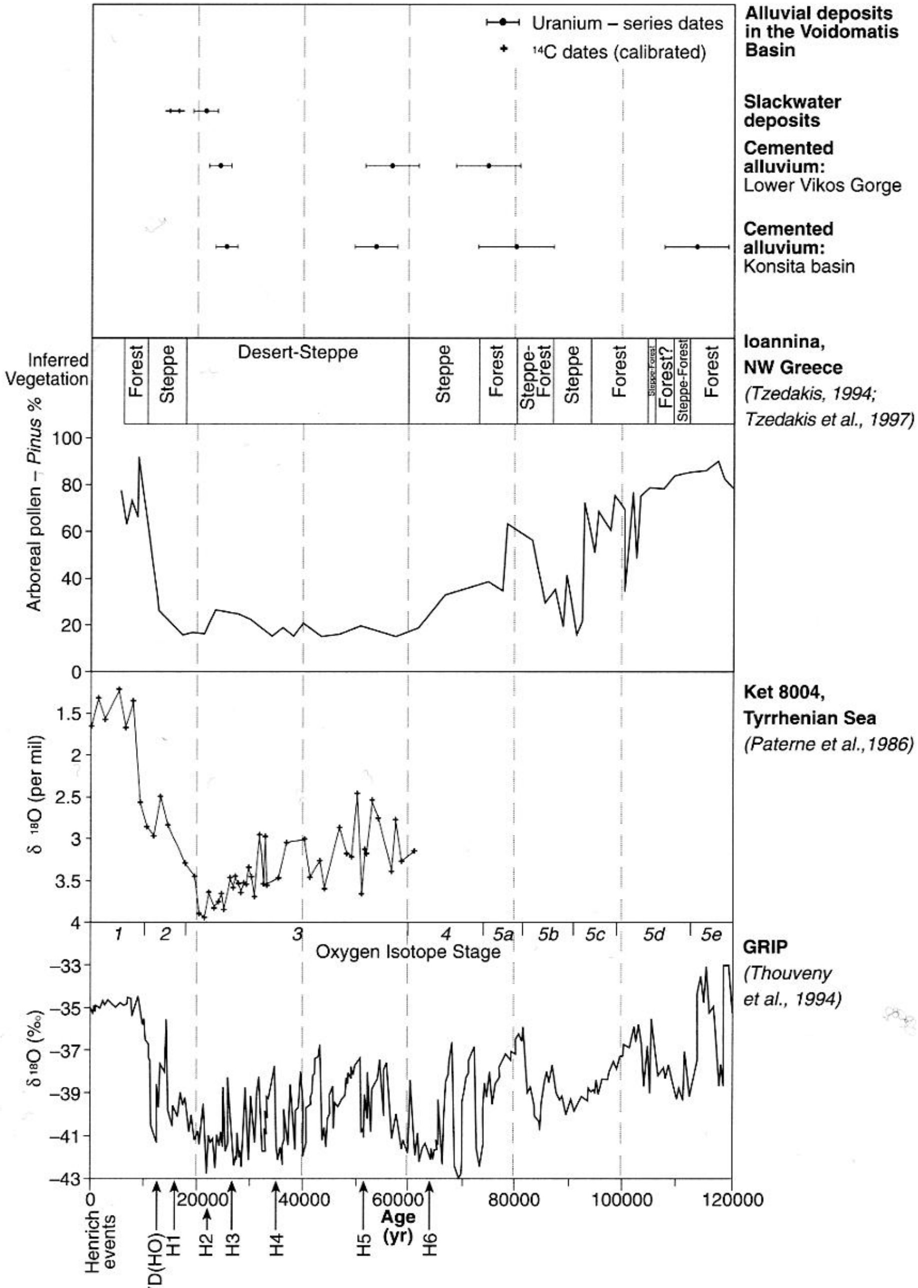

Figure 25.4 Climate proxy records and dating results from alluvial deposits in the Voidomatis basin. All results are shown in calendar years, with 2 sigma uncertainties. Radiocarbon dates, when too old for dendrochronological calibration, have been calibrated according to the results of Bard *et al.* (1990, 1992)

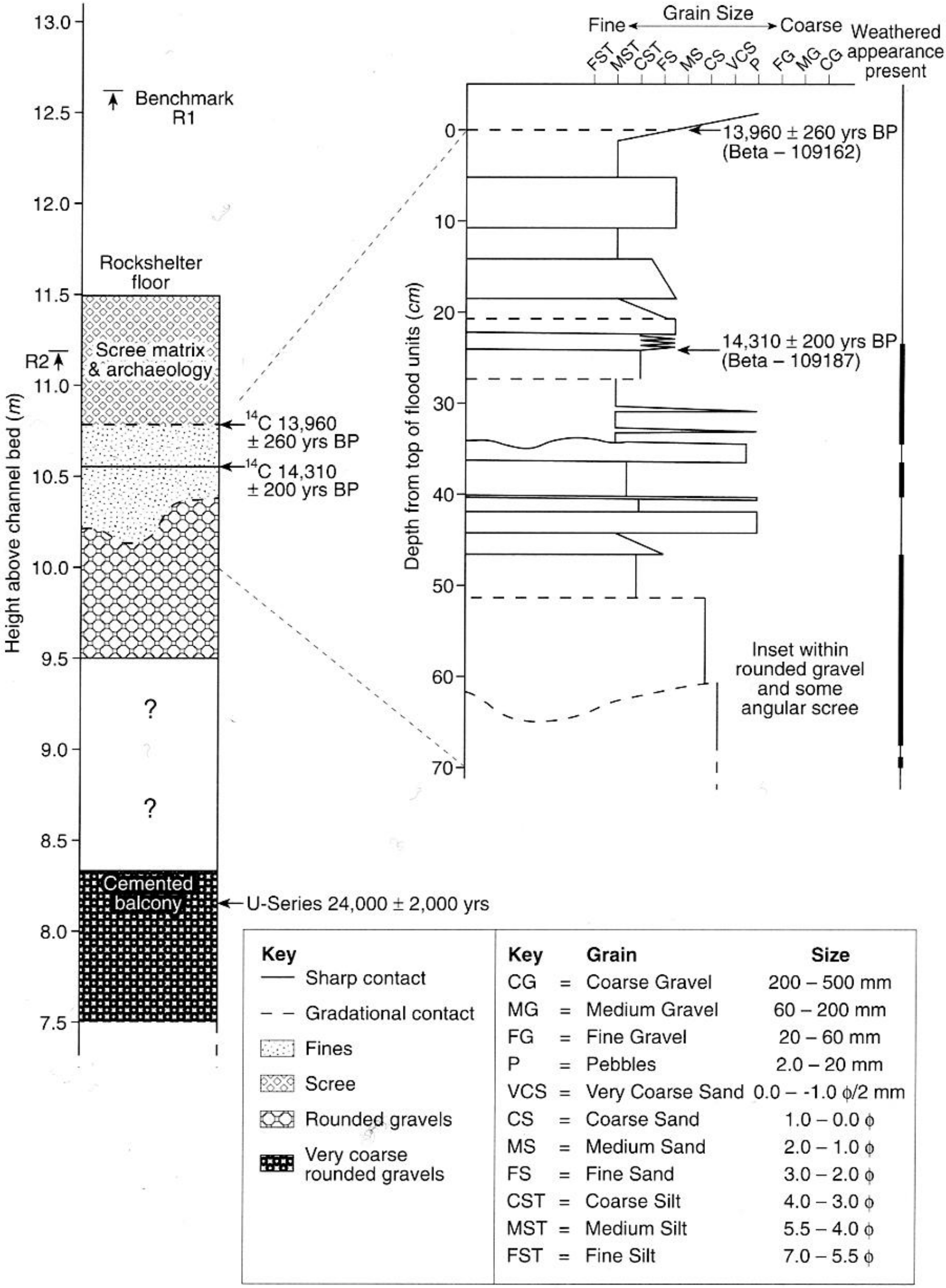

Figure 25.5 Sedimentary log of the Boila rockshelter sequence, showing the detailed stratigraphy of the palaeoflood slackwater deposits. (Conventional ^{14}C ages are shown with 2 sigma uncertainties)

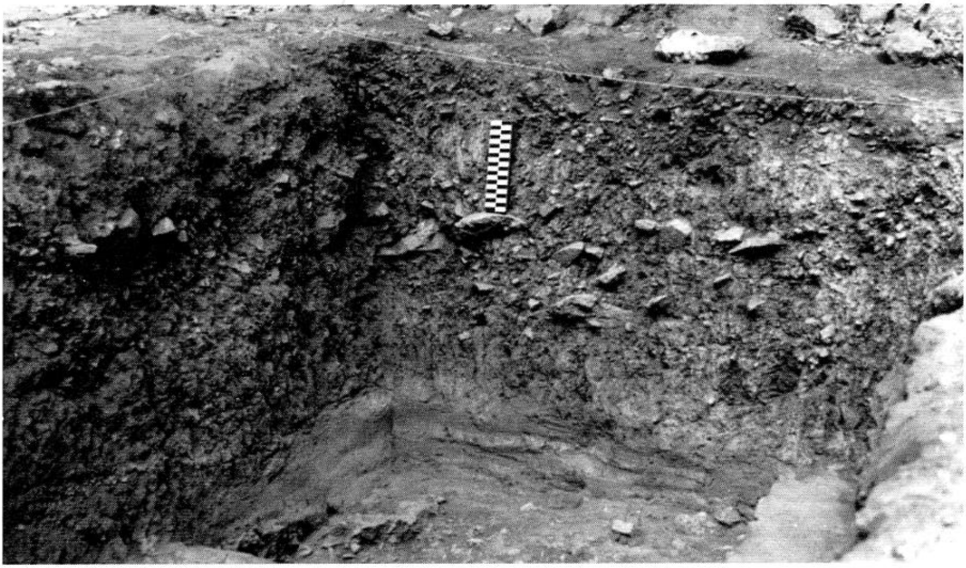

Figure 25.6 The upper metre of deposits excavated in the Boila rockshelter. The laminated slackwater deposits are clearly visible at the base of the section beneath the angular scree sediments

the LGM (Figure 25.4). Unfortunately, we have been unable to directly date the other SWD at the Old Klithonia Bridge site due to the absence of any preserved organic material for ^{14}C or cemented horizons for uranium-series. However, previous dating results (see Macklin *et al.*, 1997: 359) and its stratigraphic position in relation to a dated sequence indicate that these sediments were deposited after a phase of LGM aggradation (*c.* 25 000 ± 2000 years BP), but probably no later than the flood sediments at Boila (*c.* 14 000 years BP).

In summary, uranium-series and ^{14}C dating techniques have allowed the timing of Late Pleistocene aggradation and high-magnitude flooding within the Voidomatis basin to be established. However, as we have noted, information on fine sediment provenance has the potential to enhance our understanding of long-term fluvial activity and catchment sediment dynamics. We now describe how quantitative sediment fingerprinting can be applied as a tool to elucidate temporal changes in fluvial sediment source, and link changing catchment characteristics to the genesis of these deposits.

FINGERPRINTING PROCEDURE

The methodology, which builds on previous fingerprinting approaches (e.g. Yu and Oldfield, 1989, 1993; Walling *et al.*, 1993; Collins *et al.*, 1997a, 1998), has three key stages:

Stage 1: Theoretical Framework

There are several key assumptions associated with our approach:

(1) Variations in the properties of the fine sediment transported through the fluvial system reflect changing catchment characteristics and associated changes in sediment supply.
(2) Such catchment changes may be brought about by the influence of various environmental controls (e.g. climate and vegetation change, tectonics and land-use change) and their variation through time.

Two main potential source areas of fine sediment have been identified in the Voidomatis basin (Woodward *et al.*, 1992). First, in the east of the catchment is a high, mountainous area dominated by Jurassic to Eocene limestone. This area was glaciated during the Pleistocene and extensive moraines are present in the headwater area of Tsepelovon (Figure 25.1) (Woodward *et al.*, 1995; Smith *et al.*, 1998). Secondly, to the south is a low-lying Late Eocene to Miocene flysch basin (beds of sandstones intercalated with softer fissile siltstones) (Figure 25.1) (Bailey *et al.*, 1997). This material is highly erodible and currently exhibits a dissected semi-badland topography. Major variations in sediment source during both the Pleistocene and Holocene are therefore likely to be marked by changes in the proportion of flysch- or limestone-derived material in the fluvial sedimentary record.

Stage 2: Selection of a Suite of Variables which Together Differentiate Unequivocally all the Potential Sediment Sources

It is important to select an appropriate combination of sediment properties to effectively differentiate between all potential sediment sources. A range of statistical procedures are therefore employed in three steps.

(i) Non-parametric Kruskal–Wallis H-test to Determine which Parameters Successfully Differentiate the Source Groups

Using geological maps, air photographs, field data and XRD (X-ray diffraction) information, seven distinct geological source groups were identified (Table 25.1). In addition, alluvium is also assumed to be a potential source, thus allowing for the possible incorporation of reworked sediments. Alluvium source samples were only taken from Late Pleistocene deposits, as the more recent alluvial sediments would not have been present when most of the target samples were deposited (*c.* 113 000–14 000 years BP). The lithologies which most commonly outcrop in the catchment, namely limestone and flysch, demanded a larger number of source samples to ensure that they were adequately represented (Table 25.1). The collection of only a single dolomite sample was due to difficulty in differentiating it from limestone in the field, and its generally limited outcrop in the catchment (Figure 25.1).

All analytical data were initially made dimensionless, dividing the values for each parameter by the maximum recorded value. This was done to normalise the data,

Table 25.1 List of geological source groups used in the fingerprinting analysis

Geological source group	No. of samples
Limestone	13
Till	4
Flysch	18
Dolomite-enriched flysch	2
Dolomite	1
Ophiolite	3
Terra rossa	4
Reworked alluvium	7

thereby ensuring that each parameter exerted an equal influence in the fingerprinting calculations (Verrucchi and Minisale, 1995). A non-parametric test was used as the data were found to have neither uniform distributions nor equal variances, thus making parametric tests unsuitable. Kruskal–Wallis H-tests were employed to determine those elements which significantly differentiate between these eight source groups.

With the exception of $\chi_{FD}\%$, all parameters produce values for H_{calc} greater that H_{crit} at the 99.9 percent significance level (Table 25.2). This means that for all parameters apart from $\chi_{FD}\%$ there is a 99.9 percent probability that the differences between the mean parameter values for each source group are not attributable to random variation. This exceptionally high level of significance is due to the distinct differences between the geological source groups, which will encourage accurate

Table 25.2 Results of Kruskal-Wallis *H*-tests on the different parameters used to differentiate geological sources. Critical values are also shown. (A calculated value greater than the critical value indicates that the null hypothesis can be rejected, and the parameter does statistically significantly differentiate source groups)

Parameter	*H*-value
Barium (Ba)	45.18
Chromium (Cr)	46.65
Copper (Cu)	38.22
Lanthanum (La)	39.29
Neodymium (Nd)	38.82
Nickel (Ni)	46.67
Lead (Pb)	45.46
Rubidium (Rb)	44.98
Strontium (Sr)	44.96
Vanadium (V)	43.61
Yttrium (Y)	47.55
Zinc (Zn)	45.11
Zirconium (Zr)	47.78
Mass-specific magnetic susceptibility (χ)	43.02
% frequency-dependent magnetic susceptibility ($\chi_{FD}\%$)	14.30

H_{crit} = 14.07 (95%), 24.32 (99.9%).

fingerprinting results. The H-value for $\chi_{FD}\%$ is less than the 99.9 percent significance level, as it is not so successful at differentiating the sources, due to the low concentration of ultrafine superparamagnetic grains in these samples. Frequency-dependent magnetic susceptibility is therefore rejected at this point. In contrast, low-frequency magnetic susceptibility provided effective discrimination and has been shown to be the most reliable mineral magnetic parameter in experimental evaluations of quantitative fingerprinting procedures (Lees, 1997). All the geochemical (XRF) parameters and the low-frequency magnetic susceptibility pass the test and are used in the next stage.

(ii) Assess Parameters for Reproducibility and Long-term Stability in Geological Sediments

To produce accurate results it is important that the geochemical and magnetic data are reliable and reproducible. To assess this, repeat analyses of the same sample aliquot were carried out on a random 10 percent selection from the total sample set. The replicate data were divided by their mean, and a weighting (1 minus the standard deviation) was calculated (Table 25.3). This provides an assessment of the reproducibility of analytical measurements (Collins *et al.*, 1997a). Table 25.3 shows that all elements show very good reproducibility with the exception of La, and in particular Nd. It is well known that under certain conditions, some trace elements can be prone to alteration in sediments, often due to diagenetic effects (e.g. Farmer and Lovell, 1984). However, we have selected a combination of trace elements for this study that would be expected to be stable in this environment over the timescale of interest. Nevertheless, both La and Nd are Light Rare Earth Elements (LREE), and known to sometimes be prone to long-term instability in sediments. This could be a problem if their primary concentrations in old alluvial sediments have been altered. For reasons of both poor reproducibility and potential long-term instability, La and Nd were therefore discarded at this stage.

Table 25.3 Weightings for geochemical parameters used to differentiate geological sources. A higher weighting indicates greater analytical reproducibility

Parameter	Weighting
Sr	0.976
χ	0.972
Zn	0.958
Ni	0.956
Zr	0.950
Y	0.947
Cr	0.934
Rb	0.930
Cu	0.927
Ba	0.860
V	0.829
Pb	0.822
La	0.572
Nd	0.219

(iii) Multivariate Discriminant Analysis (MDA) to Select the Composite Fingerprint Parameters

From the parameters that pass Stages 2(i) and 2(ii), MDA is used to select a number of parameters whose combined signatures are capable of successfully differentiating all the source samples. Stepwise selection is achieved by the minimisation of Wilk's lambda, through the parameter with the smallest lambda value being selected at each step. Lambda values close to zero indicate that within-group variability is small compared to total variability, therefore good parameters and composite signatures will be associated with low lambda values.

The results of this process are shown in Table 25.4. Note that due to the very high efficiency of the parameters in differentiating the source groups, very low lambda values are obtained early in the selection process. With only the first four parameters all the source samples are correctly classified (Table 25.4) and this could be used as the composite fingerprint. However, a larger numbers of parameters with contrasting behaviour will improve the reliability of the results (Walling *et al.*, 1993), given the large number of source groups in this study (Table 25.1). With successive parameters added, there is a continued decrease in Wilk's lambda (Table 25.4), which demonstrates the improved discrimination that a larger composite fingerprint affords. Nine parameters (Table 25.4) were therefore selected as the composite fingerprint for this study. XRF and low-frequency magnetic susceptibility data allowed us to effectively differentiate between a range of diverse catchment sources. This could not have been achieved using standard mineralogical analyses such as XRD.

Stage 3: Application of a Multivariate Mixing Model to Determine Quantitative Sediment Source Composition

A similar mixing model approach is taken here to Walling *et al.* (1993). In a linear model it is assumed that the analytical results of the sediment samples are attributable to the relative contributions of the different source groups:

$$B_t = \sum_{s=1}^{S} V_{st} P_s \tag{25.1}$$

Table 25.4 Results of multivariate discriminant analysis (MDA) selection of the composite fingerprint

Parameter	Wilk's lambda	% of samples correctly classified
Cr	0.00789	75.00
χ	0.0000809	75.00
Zr	0.00000449	98.08
Ba	0.000000418	100.00
Sr	0.000000106	100.00
Y	0.0000000679	100.00
Rb	0.0000000312	100.00
Cu	0.0000000141	100.00
V	0.00000000963	100.00

subject to the following set of linear constraints:

$$\sum_{s=1}^{S} P_s = 1 \tag{25.2}$$

$$0 \leq P_s \leq 1 \tag{25.3}$$

while minimising the error term,

$$E = \sum_{t=1}^{T} \left\{ \left[B_t - \left(\sum_{s=1}^{S} V_{st} P_s \right) \right] / B_t \right\} W_t \tag{25.4}$$

where P_s is the fraction of sediment derived from source type s, V_{st} is the average value of fingerprint property t for source type s, S is the number of source types, B_t is the deposit fine sediment sample value for fingerprint property t, W_t is the weighting for fingerprint property t (Table 25.3), and T is the number of fingerprint properties considered. At the start, the source contributions P_s are set equal and the error term E is calculated. Changes in P_s are carried out that minimise E. This proceeds until no further reduction of E is possible; the change is then halved, and the procedure repeated until the optimum estimate (minimum E) for relative source contributions is achieved (cf. Walling *et al*., 1993). The values of P_s are therefore used to provide the sediment source results as a percentage value.

Part of the mixing model procedure can be illustrated by comparing the fingerprinting results to the raw XRF and mineral magnetics data. If the mixing model is operating correctly, those samples that are predicted to be dominated by a certain

Table 25.5 Mean source material fingerprint properties for the eight source groups. (Geochemical data are shown in ppm, whilst magnetic susceptibility (χ) is in $10^{-8} m^3 kg^{-1}$. The percent coefficient of variance is also shown)

Fingerprint property		Limestone	Till	Flysch	Dolomite-enriched flysch	Dolomite	Ophiolite	Terra rossa	Reworked alluvium
Ba	Mean	38	118	302	1034	964	25	429	132
	% CV	59.3	22.1	20.7	32.9		18.4	6.2	71.8
Cr	Mean	7	48	265	97	13	2831	454	47
	% CV	38.6	29.3	18.8	66.7		4.5	37.8	26.7
Cu	Mean	9	24	35	56	16	19	89	24
	% CV	34.9	6.6	48.2	57.0		3.5	27.1	18.8
Rb	Mean	3	26	88	68	11	1	103	19
	% CV	28.7	20.4	48.6	52.7		41.6	7.1	19.2
Sr	Mean	538	482	178	971	203	0	121	514
	% CV	38.3	10.6	31.2	35.3		0.0	57.2	4.9
V	Mean	14	36	120	69	14	72	141	33
	% CV	37.2	27.1	38.2	57.0		12.3	14.4	18.9
Y	Mean	4	11	23	15	11	0	63	9
	% CV	65.3	6.1	22.0	35.9		0.0	17.0	11.6
Zr	Mean	0	32	148	39	12	2	204	13
	% CV	0.0	30.2	16.2	97.0		39.9	16.2	43.7
χ	Mean	1.5	3.6	12.8	19.1	1.4	50.1	261.3	5.6
	% CV	133.9	4.3	28.6	52.6		33.5	10.4	72.3

lithology should exhibit similar geochemical and magnetic characteristics to that source type. The main sediment sources have a number of distinctive characteristics. For example, the limestone is high in Sr, but low in most other parameters (Table 25.5). The till is similar to the limestone, with a slightly less pure trace-element geochemistry reflecting the incorporation of a minor flysch component (Table 25.5). The flysch, in contrast, shows relatively high concentrations of Ba, Cr, Rb, V and Zr, and has a higher magnetic susceptibility (Table 25.5). As an example of these contrasts and the mixing model process, Figure 25.7 shows the output for two samples: one alluvial fine matrix sample predicted to have a high limestone and till content (V65a); and one SWD sample from Boila predicted to have a high flysch content (OKB1.9). These are compared to the Cr, Sr and χ data, which depict some of the clear differences between these major source groups. A comparison of the data for both samples shows that the fingerprinting predictions are consistent with the geochemical and mineral magnetic signatures, thus providing a simple qualitative check that the mixing model is producing consistent results.

RESULTS AND DISCUSSION

Phases of Aggradation and Incision

Figure 25.8 shows the fingerprinting results for contemporary fluvial fine sediments and the dated alluvial units identified in the main study reach (Figure 25.3). The recent sediments in the catchment (contemporary channel-bed fines and historical floodplain overbank sediments) have a large proportion of flysch-derived sediment. In particular, recent floodplain alluvium is calculated as having an almost 80 percent flysch origin. This undoubtedly reflects the highly erodible nature of the flysch lithology, which shows many signs of intense erosion today. In comparison, the sediments deposited around the cold period of the LGM have very different characteristics, being completely dominated by limestone and till (Figure 25.8). This dramatic contrast in sediment provenance is due to the influx of large amounts of fine sediment produced by glacial erosion in the limestone-dominated mountain headwaters. Frost weathering processes on the gorge walls may also have contributed to the limestone sand fraction of the fine sediment load during cold, glacial phases. These glacial sediment sources appear to have overwhelmed sediment supplied from the flysch slopes at this time.

The alluvial unit dated at 53 000 ± 4000 years BP has a very similar fine sediment provenance signature to that of sediments at the LGM, and can therefore also be interpreted as having been deposited during a cold phase climate. Although the unit dated at 80 000 ± 7000 years BP shows a significant proportion of dolomite, this must be treated with caution considering the low number of dolomite source samples (Table 25.1). It is more significant to note that limestone still dominates the fine fraction, being five times larger than the flysch proportion, and therefore at this time the catchment must also have been experiencing cold phase climate conditions.

The valley fill sediments dated to 113 000 ± 6000 years BP have very different characteristics, with high levels of flysch and reworked soil material. These sediments

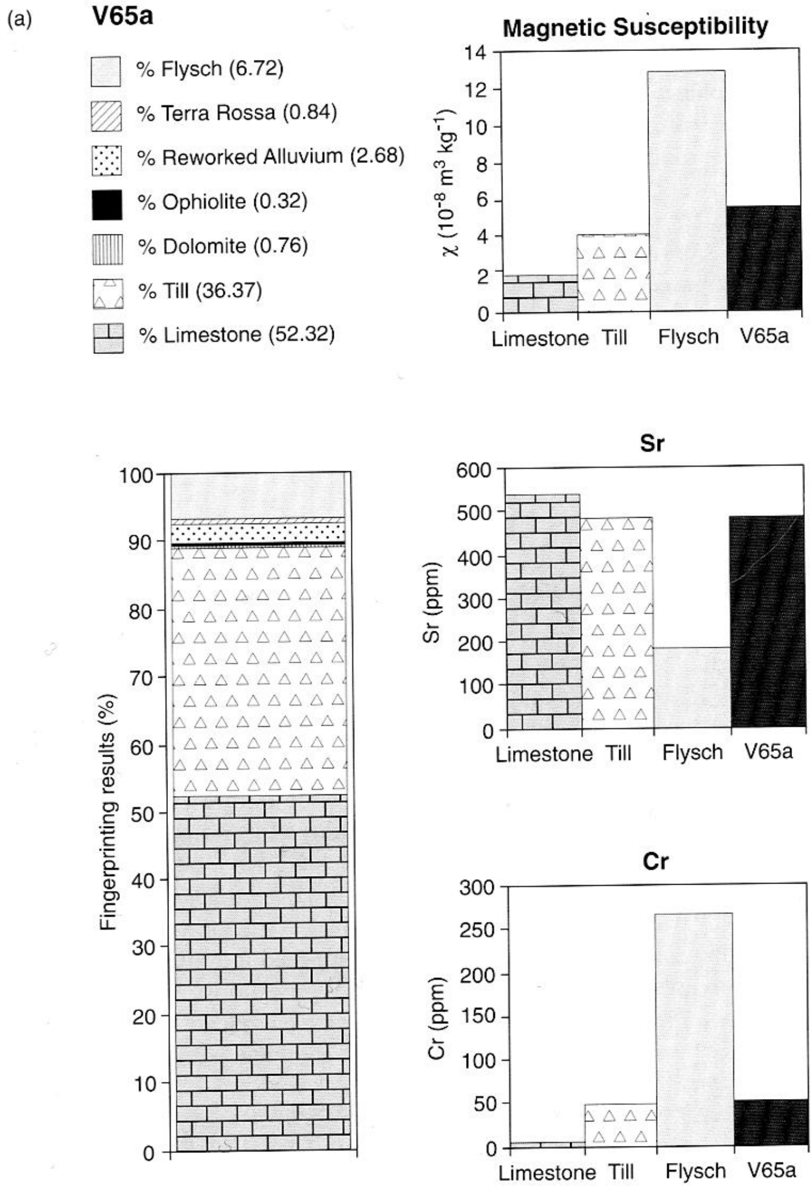

Figure 25.7(a) Comparison of fingerprinting results with geochemical and magnetic data for (a) sample V65a, which was taken from the fine-grained matrix of a coarse-grained alluvial unit, and (b) sample OKB1.9, which was taken from the Boila rockshelter SWDs

are likely to have been deposited during cool OIS 5d, following the last interglacial (OIS 5e) (Figure 25.4). The extensive thickness of these sediments (Figure 25.3), and their dominantly limestone-derived coarse gravel lithofacies, points to a period of very high sediment supply, which could not have taken place during the warm, densely vegetated environment of the OIS 5e interglacial (Tzedakis, 1994). The high proportion of *terra rossa*, the weathered soil that occurs on the limestone, suggests that it was

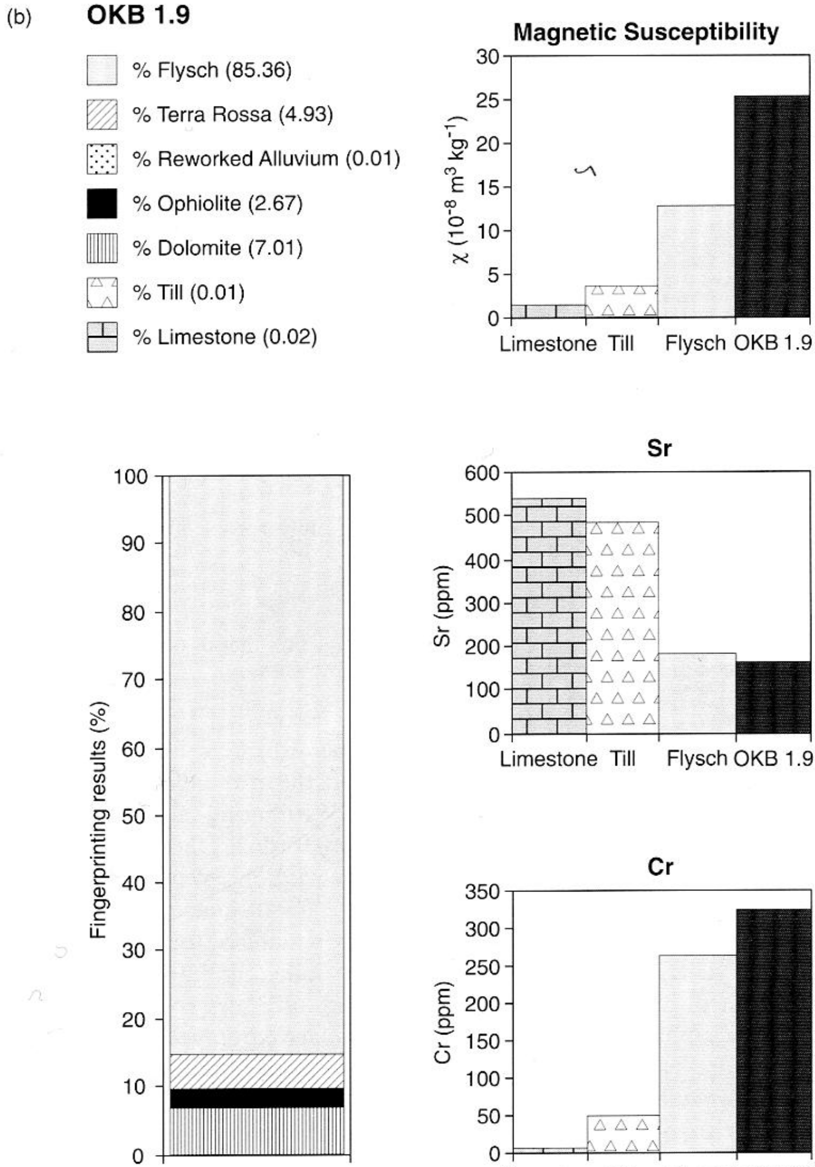

Figure 25.7(b)

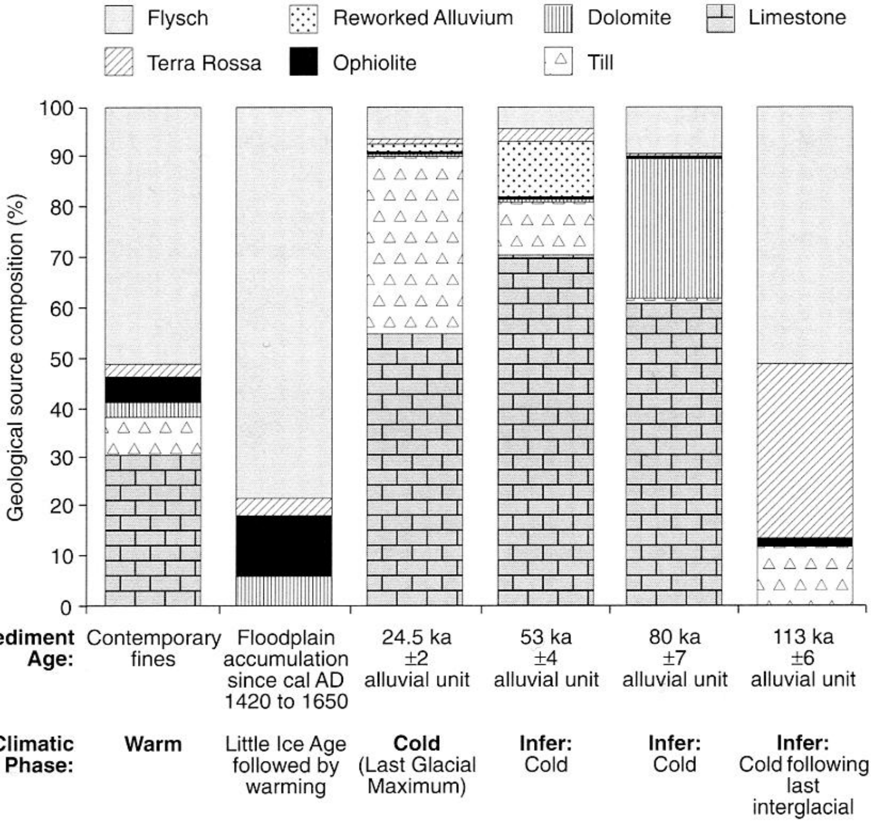

Figure 25.8 Sediment fingerprinting results from the fine matrix of dated valley fill units. (Chronological and proposed climatic information are also shown)

more widespread in the catchment at this time, which is likely considering the potential for extensive soil development during the prolonged warm interglacial conditions (van Andel and Tzedakis, 1996). Weathering and soil development would also have occurred on the flysch outcrops. However, the rapid climatic deterioration of OIS 5d brought a large decrease in vegetation cover over this part of the Balkans (Tzedakis, 1993, 1994). This would have caused slope destabilisation, releasing the pre-existing *terra rossa* and weathered flysch material for entrainment into the fluvial system. These large volumes of flysch and soil could have dominated the fine fraction, whilst the cold OIS 5d conditions would have seen frost weathering of the gorge walls to supply the dominantly limestone-derived gravel that is found in this unit. In addition, flysch erosion at this time might have been encouraged by tectonic uplift, inducing gully incision into this softer lithology. It is also possible that the predicted *terra rossa* component could in part be a secondary signal, having developed from in-situ weathering of these sediments. Establishing the significance of any diagenetic effects would require further mineral magnetic and/or microscopic analysis.

In summary, sediment fingerprinting has proved particularly useful in interpreting the history of fluvial activity. Extensive aggradation during the Late Pleistocene has occurred during periods of cold phase climate. Catchment conditions at OIS 5d, the first cool phase following the last interglacial, were very different in comparison with subsequent phases of deposition, with the fine sediment flux dominated by reworked flysch and soil material. Following that period, geomorphological processes supplying fine sediment from the limestone and till area became dominant during cold Late Pleistocene phases. The volume of flysch-derived sediment runoff probably actually increased during these cold periods, as the low vegetation cover would have made the flysch slopes unstable and susceptible to gully and wash erosion. However, the relative contribution of flysch to the units deposited at *c.* 25 000, 55 000 and 78 000 years BP is suppressed to only *c.* 10 percent (Figure 25.8), which suggests that the volume of flysch-derived material was simply swamped by a vast increase in the volume of sediment supply from glacial erosion and mechanical rock breakdown in the mountainous limestone areas. The evidence for this sediment source change reflecting a considerable increase in sediment delivery is corroborated by the fact that this limestone-dominated sediment fingerprint is found in such thickly aggraded alluvial units. The large increase in sediment supply during cold phases was almost certainly a key stimulus for these periods of aggradation. This demonstrates the large impact of glaciation and cold climate weathering upon this river system during the Late Pleistocene (Woodward *et al.*, 1995). Following cold glacial periods, progressive incision has followed the decline in glacial sediment inputs and the stabilisation of slopes by increasing vegetation density (Turner and Sánchez Goñi, 1997; Willis, 1997). This incision has dominated the post-glacial period, with the only significant phase of aggradation occurring during the Late Holocene following an increase in fine sediment supply from flysch areas and the vertical accretion of the Klithi-type sediments (Lewin *et al.*, 1991).

Periods of high-magnitude flooding

In Figure 25.9 the average source characteristics of several bulk samples taken from sedimentary units within each SWD are shown, with the fingerprints for sediments deposited during warm and cold phase climates included for reference. The SWDs at Boila show very similar characteristics to the sediments that are typical of the modern warm phase climate, with a large proportion of flysch and very little limestone or till. This would suggest that at *c.* 14 000 years BP, when these flood sediments were deposited, glacial sediment inputs were not significant and that environmental conditions may have been similar to those today. However, the characteristics of the sediments in both the Old Klithonia Bridge and Tributary SWDs are very different, with the dominance of limestone and till being comparable to that of the alluvial unit deposited at the LGM. This suggests cold phase deposition of these flood sediments, which is consistent with the date of 21 250 ± 2500 years BP at the Tributary site. Although the timing of deposition at the Old Klithonia Bridge site is not exactly constrained, the sediments show very similar source characteristics to the Tributary site and, given their stratigraphic context discussed above, may therefore have been deposited at a similar time. The results confirm that these floods were not contemporaneous with those which deposited the sediments at Boila. Therefore, even

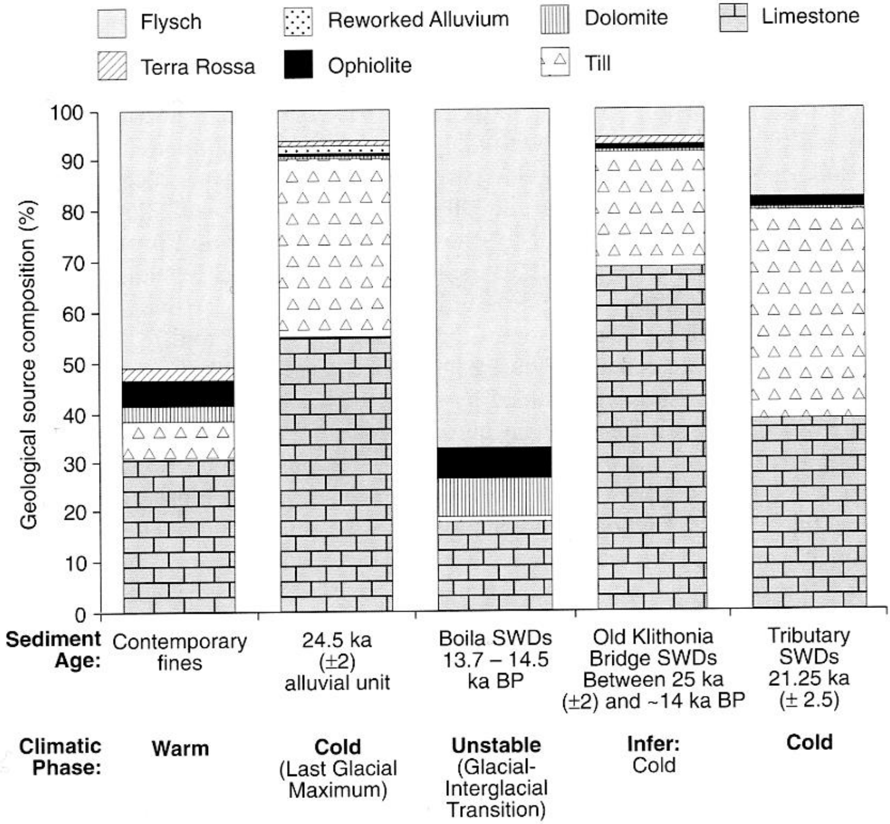

Figure 25.9 Sediment fingerprinting results from the palaeoflood slackwater deposits. (Chronological and proposed climatic information are also shown)

without being able to obtain precise dates for all these deposits, the fingerprinting results enable an interpretation of the timing and the type of environment during which the sediments were deposited. This method shows the considerable potential for provenancing work on SWDs. It is perhaps surprising that the only previous SWD provenance study of note is that of Saynor and Erskine (1993), who successfully employed heavy mineral analysis to differentiate flood sediments from those which contained a proportion of locally derived colluvium. In future work we aim to look in more detail at the provenance of individual flood units within these SWDs. This promises to enable sediments from different flood events to be distinguished with confidence, and to facilitate palaeoenvironmental interpretation of the entire SWD sequences (some of which are over 2.5 m in thickness). In this study, the fingerprinting data provide evidence for two separate periods of high-magnitude flooding during the Late Pleistocene. Extreme flooding around the LGM, represented by SWDs at the Tributary and Old Klithonia Bridge sites, would have coincided with high sediment availability, and would therefore have been important for river aggradation around the LGM (cf. Bull, 1979, 1988). The presence of coarse gravels and small boulders in this LGM alluvial unit also points to high discharges. Such floods probably resulted from intense glacial meltwater in spring. The floods which deposited sediment in Boila, however, occurred during the Late-glacial period where the delivery of limestone-rich glacially comminuted fines had waned, suggesting a reduction in sediment supply and more stable, vegetated slopes (Turner and Sánchez Goñi, 1997). These later floods, occurring at a time of lower sediment availability, may therefore have resulted in considerable incision through the Late Pleistocene deposits (cf. Bull, 1979, 1988).

Reliability of Fingerprinting Results

It is important to assess the reliability of the fingerprinting results. The most extensive lithologies within the catchment (limestone, flysch and till) dominate the fingerprinting predictions, which suggests that the results are realistic. The results are also in accord with previous work based on semi-quantitative XRD analyses (Woodward *et al.*, 1992). However, the difference between measured and predicted parameter values can be used to obtain a mean relative error. In this study these are typically ± 10–15 percent, which is only slightly higher than recent work on contemporary suspended sediments (*c.* ± 10 percent) reported by Collins *et al.* (1997a, 1998). This is encouraging considering some of the potential problems involved in determining provenance over long timescales. However, it is important to appreciate that this is only a crude estimate of error that is partly influenced by between-parameter co-correlation. Further work is required into the improved quantification of fingerprinting uncertainty (e.g. Rowan *et al.*, see Chapter 14).

We have tested the results by comparing the fingerprinting predictions with independent mineralogical data determined by XRD. The distinctive characteristics of the main sediment sources (Table 25.5) reflect their mineralogical differences. The limestone has relatively simple geochemical and mineral magnetic characteristics as it is composed largely of calcite with small amounts of quartz. The till is similar to the limestone, dominated by calcite but including a little more quartz and feldspar. In contrast, high concentrations of many trace elements in the flysch, and its higher magnetic susceptibility, can be explained by a mineralogy dominated by quartz, with a significant amount of feldspar and various clay minerals. As an example, Figure 25.10 shows the mineralogical data for the two samples whose fingerprinting results are displayed in Figure 25.7. For V65a (Figure 25.10) the mineralogy is dominated by calcite, with some quartz but very little clays or feldspar, thus supporting the fingerprinting predictions of approximately 90 percent limestone and till. The agreement of the data is also encouraging for OKB1.9 (Figure 25.10), which has a high quartz content and a significant amount of feldspar and clays, which is consistent with the high flysch content predicted for this sample. Thus in both cases, mineralogical information fully supports the fingerprinting predictions, suggesting that the source ascription is both accurate and reliable.

Nevertheless, there are a number of potential problems associated with fingerprinting Late Pleistocene sediment:

(1) Diagenesis is a potential source of inaccuracy. We have attempted to minimise diagenetic effects through careful sampling to avoid weathered deposits, as well

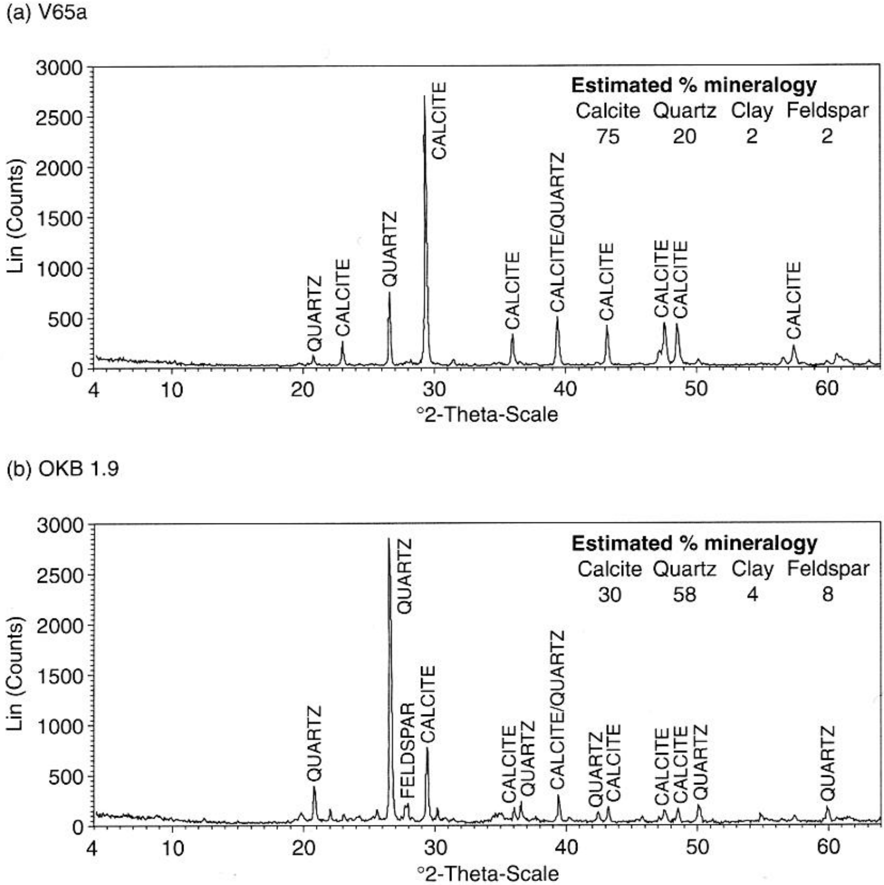

Figure 25.10 Mineralogical characteristics of samples V65a and OKB1.9. The fingerprinting results for these samples are shown in Figure 25.7

as choosing geologically stable fingerprinting parameters. However, this could be explored further through more detailed mineral magnetic or microscopic analysis.

(2) It is difficult to correct for potential grain-size effects when some of the principal sediment sources are bedrock. Therefore, analysis of standardised fine sediment fractions (powdered <2 mm for XRF, <1 mm for magnetics) was judged to be appropriate.

With these possible sources of error in mind, these results demonstrate the potential of quantitative sediment fingerprinting over Late Pleistocene timescales. Quantitative fine sediment provenancing is a valuable complement to other approaches for the investigation of long-term river behaviour, and offers considerable promise for the interpretation of slackwater sediments.

CONCLUSIONS

(1) A quantitative fingerprinting technique has been successfully applied over long timescales (10^2–10^5 years).

(2) Quantitative information on sediment sources corroborates the radiometric dating results to facilitate a fuller interpretation of Late Pleistocene alluvial history. The approach provides detailed evidence of the changes in sediment delivery processes caused by environmental variations. It has been demonstrated that in the Voidomatis basin, sediment sources have been strongly influenced by climatic controls. Quantitative sediment fingerprinting can therefore be a valuable tool for interpreting long-term river activity.

(3) In the Voidomatis basin, dating of cemented alluvial deposits has been successfully achieved by uranium-series techniques. Extensive river aggradation has occurred over the Late Pleistocene in at least four separate periods, with the cessation of deposition dated to approximately 113 000, 78 000, 55 000 and 25 000 years BP. Fingerprinting results demonstrate that these periods of deposition occurred during a cold phase climate, almost certainly as a result of increased sediment supply from glacial erosion, with a minor contribution from frost weathering processes. This builds considerably on previous work in the area (Lewin *et al.*, 1991), to further demonstrate the dynamic nature of Late Pleistocene river development in Mediterranean mountain environments.

(4) Evidence has been presented for high-magnitude flooding during both glacial (*c.* 21 000 years BP) and Late Glacial (*c.* 14 000 years BP) environments. Such palaeoflood events have played an important role in the Quaternary development of the Voidomatis River. Quantitative sediment fingerprinting is particularly valuable for interpreting palaeoflood slackwater deposits.

ACKNOWLEDGEMENTS

This work was carried out whilst R.H. was in receipt of a Departmental PhD Studentship from the School of Geography, University of Leeds. J.W. and M.G.M. acknowledge the support of NERC Grant GR9/2916. The authors are indebted to Claire Sedgwick for her assistance with the majority of the fieldwork and for many helpful discussions. Adrian McDonald is thanked for his valuable comments. Damien Lanforth and Clair Calvert-Smith provided much assistance with XRF analysis. Simon Robinson is thanked for his helpful advice and for allowing R.H. access to laboratories at the School of Geography, University of Manchester. Beta Analytic Inc. carried out the radiocarbon analysis. IGME (Athens) provided research permits and sample export licences. Eleni Kotjaboupoulou kindly allowed us access to the deposits at Boila. Adrian Harvey and Tim Quine are both thanked for their valuable reviews of this chapter. Finally, we are also grateful for the excellent work of the Graphics Department in the School of Geography, University of Leeds.

REFERENCES

Baker, V. R. 1977. Stream channel response to floods, with examples from central Texas. *Geological Society of America Bulletin*, **88**, 1057–1071.

Baker, V. R. and Pickup, G. 1987. Flood geomorphology of the Katherine Gorge, Northern Territory, Australia. *Geological Society of America Bulletin*, **98**, 653–646.

Baker, V. R., Kochel, R. C., Patton, P. C. and Pickup, G. 1983. Paleohydologic analysis of Holocene flood slack-water sediments. *Special Publications of the International Association of Sedimentology*, **6**, 229–239.

Bailey, G. N., Turner, C., Woodward, J. C. Macklin, M. G., and Lewin, J. 1997. The Voidomatis Basin: an introduction. In Bailey, G. N. (ed.) *Klithi: Palaeolithic Settlement and Quaternary Landscape in Northwest Greece. Volume 2: Klithi in Its Local and Regional Setting*. McDonald Institute, Cambridge, 321–346.

Bard, E., Hamelin, B., Fairbanks, R. G. and Zinder, A. 1990. Calibration of the ^{14}C timescale over the past 30,000 years using mass spectrometric U–Th ages from Barbados corals. *Nature*, **345**, 405–410.

Bard, E., Fairbanks, R. G., Arnold, M. and Hamelin, B. 1992. ^{230}Th/^{234}U and ^{14}C ages obtained by mass spectrometry on corals from Barbados (West Indies), Isabela (Galapagos) and Mururoa (French Polynesia). In Bard, E. and Broecker, W. S. (eds) *The Last Deglaciation: Absolute and Radiocarbon Chronologies*. Springer-Verlag: Berlin, Heidelberg, 103–110.

Benito, G., Machado, M. J., Pérez-González, A. and Sopeña, A. 1998. Palaeoflood hydrology of the Tagus River, Central Spain. In Benito, G., Baker, V. R. and Gregory, K. J. (eds) *Palaeohydrology and Environmental Change*. John Wiley, Chichester, 317–333.

Bischoff, J. L. and Fitzpatrick, J. A. 1991. U-series dating of impure carbonates: an isochron technique using total-sample dissolution. *Geochimica et Cosmochimica Acta*, **55**, 543–554.

Black, S., Macdonald, R. and Kelly, M. 1997. Crustal origin for peralkaline rhyolites from Kenya: evidence from U-series disequilibria and Th-isotopes. *Journal of Petrology*, **38**, 277–297.

Bull, W. B. 1979. Threshold of critical power in streams. *Bulletin of the Geological Society of America*, **90**, 453–464.

Bull, W. B. 1988. Floods: degradation and aggradation. In Baker, V. R. Kochel, R. C. and Patton, P. C. (eds) *Flood Geomorphology*. John Wiley, New York, 157–165.

Collins, A. L., Walling, D. E. and Leeks, G. J. L. 1997a. Source type ascription for fluvial suspended sediment based on a quantitative composite fingerprinting technique. *Catena*, **29**, 1–27.

Collins, A. L., Walling, D. E. and Leeks, G. J. L. 1997b. Use of the geochemical record preserved in floodplain deposits to reconstruct recent changes in river basin sediment sources. *Geomorphology*, **19**, 151–167.

Collins, A. L., Walling, D. E. and Leeks, G. J. L. 1998. Use of composite fingerprints to determine the provenance of the contemporary suspended sediment load transported by rivers. *Earth Surface Processes and Landforms*, **23**, 31–52.

Coxon, P., Owen, L. A. and Mitchell, W. A. 1996. A Late Pleistocene catastrophic flood in the Lahul Himalayas. *Journal of Quaternary Science*, **11**, 495–510.

Dearing, J. A. 1992. Sediment yields and sources in a Welsh upland catchment during the past 800 years. *Earth Surface Processes and Landforms*, **17**, 1–22.

Dearing, J. A. 1994. *Environmental Magnetic Susceptibility: Using the Bartington MS2 System*. Chi Publishing: Kenilworth.

De Boer, D. H. and Crosby, G. 1995. Evaluating the potential of SEM/EDS analysis for fingerprinting suspended sediment derived from two contrasting topsoils. *Catena*, **24**, 243–258.

Ely, L. L. 1997. Response of extreme floods in the southwestern United States to climatic variations in the late Holocene. *Geomorphology*, **19**, 175–201.

Ely, L. L. and Baker, V. R. 1985. Reconstructing paleoflood hydrology with slackwater deposits: Verde River, Arizona. *Physical Geography*, **5**, 103–126.

Farmer, J. G. and Lovell, A. 1984. Massive diagenetic enhancement of manganese in Loch Lomond sediments. *Environmental Technology Letters*, **5**, 257–262.

Foster, I. D. L., Lees, J. A., Owens, P. N. and Walling, D. E. 1998. Mineral magnetic characterization of sediment sources from an analysis of lake and floodplain sediments in the catchments of the Old Mill Reservoir and Slapton Ley, South Devon, UK. *Earth Surface Processes and Landforms*, **23**, 685–703.

Gillieson, D., Ingle Smith, D., Greenaway, M. and Ellaway, M. 1991. Flood history of the limestone ranges in the Kimberly region, Western Australia. *Applied Geography*, **11**, 105–123.

Greenbaum, N., Margalit, A., Schick, A. P., Sharon, D. and Baker, V. R. 1998. A high magnitude storm and flood in a hyperarid catchment, Nahal Zin, Negev Desert, Israel. *Hydrological Processes*, **12**, 1–24.

GRIP (Greenland Ice-core Project) Members 1993. Climate instability during the last interglacial period recorded in the GRIP ice core. *Nature*, **364**, 203–207.

Grimshaw, D. L. and Lewin, J. 1980. Source identification for suspended sediments. *Journal of Hydrology*, **47**, 151–161.

Gupta, A. 1983. High-magnitude floods and stream channel response. *Special Publication of the International Association of Sedimentologists* **6**, 219–227.

Haughton, P. D. W., Todd, S. P. and Morton, A. C. 1991. Sedimentary provenance studies. In Morton, A. C., Todd, S. P. and Haughton, P. D. W. (eds) *Developments in Sedimentary Provenance Studies*. Geological Society Special Publication No. 57, The Geological Society, London, 1–13.

Hutchinson, S. M. 1995. Use of magnetic and radiometric measurements to investigate erosion and sedimentation in a British upland catchment. *Earth Surface Processes and Landforms*, **20**, 293–314.

IGME, 1968. *1:50,000 Geological Map of Greece*, Doliana Sheet, Institute of Geological and Mineralogical Research, Athens.

IGME, 1970, *1:50,000 Geological Map of Greece*, Tsepelovon Sheet, Institute of Geological and Mineralogical Research, Athens.

Kochel, R. C. and Baker, V. R. 1982. Paleoflood hydrology. *Science*, **215**, 353–361.

Kochel, R. C. and Baker, V. B. 1988. Paleoflood analysis using slackwater deposits. In Baker, V. R., Kochel, R. C. and Patton P. C. (eds) *Flood Geomorphology*. John Wiley, New York, 357–376.

Kotjaboupoulou, E., Panagopoulou, E. and Adam, E. 1997. The Boila Rockshelter: a preliminary report. In Bailey, G. N. (ed.) *Klithi: Palaeolithic Settlement and Quaternary Landscape in Northwest Greece. Volume 2: Klithi in Its Local and Regional Setting*. McDonald Institute, Cambridge, 427–438.

Kurashige, Y. and Fusejima, Y. 1997. Source identification of suspended sediment from grain size distributions: I. Application of non-parametric statistical tests. *Catena*, **31**, 39–52.

Kuzucuoglu, C., Pastre, J-F., Black, S., Ercan, T., Fontugne, M., Guillou, H., Hatté, C., Karabiyikoglu, M., Orth, P. and Türkecan, A. 1998. Identification and dating of tephras from Quaternary sedimentary sequences of inner Anatolia. *Journal of Volcanology and Geothermal Research*, **85**, 153–172.

Lees, J. 1997. Mineral magnetic properties of mixtures of environmental and synthetic materials: linear additivity and interaction effects. *Geophysics Journal International*, **131**, 335–346.

Lewin, J., Macklin, M. G. and Woodward, J. C. 1991. Late Quaternary fluvial sedimentation in the Voidomatis basin, Epirus, Northwest Greece. *Quaternary Research*, **35**, 103–115.

Macklin, M. G., Lewin, J. and Woodward, J. C. 1997. Quaternary river sedimentary sequences of the Voidomatis basin. In Bailey, G. N. (ed.) *Klithi: Palaeolithic Settlement and Quaternary Landscape in Northwest Greece. Volume 2: Klithi in Its Local and Regional Setting*. McDonald Institute, Cambridge, 347–336.

O'Connor, J. E., Ely, L. L., Wohl, E. E., Stevens, L. E., Melis, T. S., Kale, V. S. and Baker, V. R. 1994. A 4500-year record of large floods on the Colorado River in the Grand Canyon, Arizona. *The Journal of Geology*, **102**, 1–9.

Oldfield, F., Maher, B. A., Donoghue, J. and Pierce, J. 1985. Particle-size related, mineral magnetic source sediment linkages in the Rhode River catchment, Maryland, USA. *Journal of the Geological Society*, **142**, 1035–1046.

Olley, J. M., Murray, A. S., Mackenzie, D. H. and Edwards, K. 1993. Identifying sediment sources in a gullied catchment using natural and anthropogenic radioactivity. *Water Resources Research*, **29**, 1037–1043.

Passmore, D. G. and Macklin, M. G. 1994. Provenance of fine-grained alluvium and late-Holocene land-use change in the Tyne basin, northern England. *Geomorphology*, **9**, 127–142.

Paterne, M., Guichard, F., Labeyrie, J., Gillot, P. Y. and Duplessy, J. C. 1986. Tyrrhenian tephrochronology of the oxygen isotope record for the past 60,000 years. *Marine Geology*, **72**, 259–285

Peart, M. R. and Walling, D. E. 1986. Fingerprinting sediment source: the example of a drainage basin in Devon, UK. *Drainage Basin Sediment Delivery*. IAHS Publication **174**. IAHS Press, Wallingford, 41–55.

Saynor, M. J. and Erskine, W. D. 1993. Characteristics and implications of high-level slack-water deposits in the Fairlight Gorge, Nepean River, Australia. *Australian Journal of Marine and Freshwater Research*, **44**, 735–747.

Smith, G. R., Woodward, J. C., Heywood, D. I. and Gibbard, P. L. 1998. Mapping glaciated karst terrain in a Mediterranean mountain environment using SPOT and TM data. In Burt, P. J. A., Power, C. H. and Zukowskyj, P. M. (eds) *R SS98: Developing International Connections*. Proceedings of the Remote Sensing Society's Annual Meeting, Greenwich, 9–11 September 1998, 457–463.

Thompson, R. and Oldfield, F. 1986. *Environmental Magnetism*. Allen & Unwin, London.

Thouveny, N., de Beaulieu, J.-L., Bonifay, E., Creer, K. M., Guiot, J., Icole, M., Johnsen, S., Jouzel, J., Reille, M., Williams, T. and Williamson, D. 1994. Climate variations in Europe over the past 140 kyr deduced from rock magnetism. *Nature*, **371**, 503–506.

Turner, C. and Sánchez Goñi, M.-F. 1997. Late glacial landscape and vegetation in Epirus. In Bailey, G. N. (ed.) *Klithi: Palaeolithic Settlement and Quaternary Landscape in Northwest Greece. Volume 2: Klithi in Its Local and Regional Setting*. McDonald Institute, Cambridge, 559–585.

Tzedakis, P. C. 1993. Long-term tree populations in northwest Greece through multiple Quaternary climatic cycles. *Nature*, **364**, 437–440.

Tzedakis, P. C. 1994. Vegetation change through glacial–interglacial cycles: a long pollen sequence perspective. *Philosophical Transactions of the Royal Society, London*, Series B, **345**, 403–432.

Tzedakis, P. C., Andrieu, V., de Beaulieu, J.-L., Crowhurst, S., Follieri, M., Hooghiemstra, H., Magri, D., Reille, M., Sadori, L., Shackleton, N. J. and Wijmstra, T. A. 1997. Comparison of terrestrial and marine records of changing climate of the last 500,000 years. *Earth Science and Planetary Science Letters*, **150**, 171–176.

Van Andel, T. H. and Tzedakis, P. C. 1996. Palaeolithic landscapes of Europe and environs, 150,000–25,000 years ago: an overview. *Quaternary Science Reviews*, **15**, 481–500.

Verrucchi, C. and Minisale, A. 1995. Multivariate statistical comparison of Northern Apennines Paleozoic sequences: a case study for the formations of the Monti Romani (Southern Tuscany–Northern Latium, Italy). *Applied Geochemistry*, **10**, 581–598.

Walling, D. E. and Woodward, J. C. 1992. Use of radiometric fingerprints to derive information on suspended sediment sources. In *Erosion and Sediment Transport Monitoring Programmes in River Basins* (Proceedings of the Oslo Symposium, August 1992), IAHS Publication **210**. 153–164.

Walling, D. E. and Woodward, J. C. 1995. Tracing sources of suspended sediment in River Basins: a case study of the River Culm, Devon, UK. *Marine and Freshwater Research*, **46**, 327–336.

Walling, D. E., Peart, M. R., Oldfield, F. and Thompson, R. 1979. Suspended sediment sources identified by magnetic measurements. *Nature*, **281**, 110–113.

Walling, D. E., Woodward, J. C. and Nicholas, A. P. 1993. A multi-parameter approach to fingerprinting suspended sediment sources. In *Tracers in Hydrology* (Proceedings of the

Yokohama Symposium, July 1993), IAHS Publication **215**, IAHS Press, Wallingford. 329–328.

Willis, K. 1997. Vegetational history of the Klithi environment: a palaeoecological viewpoint. In Bailey, G. N. (ed.) *Klithi: Palaeolithic Settlement and Quaternary Landscape in Northwest Greece. Volume 2: Klithi in Its Local and Regional Setting*. McDonald Institute, Cambridge, 395–414.

Wohl, E. E. 1992. Bedrock benches and boulder bars: floods in the Burdekin Gorge of Australia. *Geological Society of America Bulletin*, **104**, 770–778.

Wood, P. A. 1978. Fine-sediment mineralogy of source rocks and suspended sediment, Rother catchment, West Sussex. *Earth Surface Processes*, **3**, 255–263.

Woodward, J. C., Lewin, J. and Macklin, M. G. 1992. Alluvial sediment sources in a glaciated catchment: the Voidomatis basin, Northwest Greece. *Earth Surface Processes and Landforms*, **17**, 205–216.

Woodward, J. C., Macklin, M. G. and Lewin, J. 1994. Pedogenic weathering and relative-age dating of Quaternary alluvial sediments in the Pindus Mountains of Northwest Greece. In Robinson, D. A. and Williams, R. B. G. (eds) *Rock Weathering and Landform Evolution*. John Wiley, Chichester, 259–283.

Woodward, J. C., Lewin, J. and Macklin, M. G. 1995. Glaciation, river behaviour and Palaeolithic settlement in upland northwest Greece. In Lewin, J., Macklin, M. G. and Woodward, J. C. (eds) *Mediterranean Quaternary River Environments*. Balkema, Rotterdam, 115–129.

York, D. 1969. Least squares fitting of a straight line with correlated errors. *Earth and Planetary Science Letters*, **5**, 320–324.

Yu, L. and Oldfield, R. 1989. A multivariate mixing model for identifying sediment source from magnetic measurements. *Quaternary Research*, **32**, 168–181.

Yu, L. and Oldfield, R. 1993. Quantitative sediment source ascription using magnetic measurements in a reservoir-catchment system near Nijar, S.E. Spain. *Earth Surface Processes and Landforms*, **18**, 441–454.